Determination of the anisotropy complex refractive indices of chicken tissues *in vitro* at 650 nm

Ping Sun
pingsun@bnu.edu.cn

Department of Physics, Beijing Normal University, Beijing Area Major Laboratory of Applied Optics, Beijing, 100875, P. R. China

Hanxu Sun

School of Automation, Beijing University of Posts and Telecommunication, Beijing, 100876, P. R. China

The anisotropy complex refractive index of tissue is an important parameter in understanding the behavior of light, including its transportation in and interaction with tissues. We used the specular reflection method to investigate the anisotropy complex refractive index of chicken tissue with fibrous structures *in vitro* at a wavelength of 650 nm. The measurement data were highly consistent with the Fresnel equations. The results showed that the real refractive index was higher along the orientation of the fibers than along the cross section, but the imaginary refractive index was nearly identical. Furthermore, the fiber orientation was in the direction of the optic axis of the chicken tissue and the chicken tissue section was similar to a negative uniaxial crystal wafer. [DOI: 10.2971/jeos.2010.10030]

Keywords: complex refractive index, optical anisotropy, specular reflection, chicken tissue, fibrous structure

1 INTRODUCTION

Tissue characteristics play an important role in all kinds of medical laser treatments and biomedical imaging [1, 2]. Among the various optical parameters of tissues, the refractive index is an important one. Tissue is an optically turbid medium, and when photons propagate in it, they are scattered and absorbed by the particles and macromolecules inside the tissue. It is recognized that at microscopic scales ranging from 1 to 10 μm, refractive index fluctuations cause light scattering [3]. To determinate the spatial and temporal distributions of light in tissues, primarily the optical properties of tissues should be measured. For example, in a Monte Carlo simulation of photon interactions with the boundaries of a homogeneous biological tissue or interfaces within a heterogeneous tissue, the refractive index is a key parameter [4, 5]. Until now, a few attempts to derive the refractive index of biological tissues have been reported. The first attempt at measuring the refractive index in biological tissues was carried out by Bolin *et al* [6] and included a distribution measurement of the light transmitted through an optical fiber with tissue as the fiber cladding. The technique of optical coherence tomography (OCT), which uses coherent reflection inside a tissue with a converging light beam was introduced as another emerging technology [7]. Measurements of specular reflectance at one or a few incident angles based on the Fresnel equations have been employed to determine the complex refractive index for turbid samples [8, 9] and biological samples [10]–[13]. To our knowledge, the latter method is widely used to measure the refractive index of tissue. However, the challenge of determining the refractive index of biological tissues from reflectance accurately is still significant because of the presence of turbidity in tissues. Collagen and muscle fibers are common constituents of many biological tissues. Tissue birefringence results primarily from the linear anisotropy of fibrous structures that form the extracellular media [14, 15]. Recently, investiga-

tions on the optical anisotropy of fibrous tissues using OCT, especially polarization-sensitive optical coherence tomography (PS-OCT), were reported by several research groups [16]–[19]. Many tissues such as tendon, muscle, nerve, and cartilage influence the polarization state of light backscattered due to their linear or fibrous structures, and PS-OCT can potentially be a very useful technique in the investigation of the structural properties and biochemical composition of these tissues. However, most of the studies on birefringence of tissue have been paid more attention to the measurement or imaging of birefringence, and little attention to the refractive index values of tissues. To understand light behavior, including its transportation in tissues and interaction with biological objects, it is necessary to acquire accurate data regarding the refractive indices of tissues. Therefore, it is still an open question and an important task to obtain anisotropy refractive index of tissue accurately.

The aim of this work was to measure the anisotropy complex refractive indices of fresh chicken tissues *in vitro* by means of a nonlinear regression of the total coherent transmittivity curve of the tissue-prism system. The anisotropy complex refractive index was obtained at a wavelength of 650 nm in accordance with the Fresnel equations. The optic axis of chicken tissue was determined with polarized light.

2 METHODS

The method of measuring specular reflection comes from the well-known classical laws of reflection and refraction. When total internal reflection occurs, the incident light does not interact with the second medium except in the region of the interface of thickness that is about the same order of magni-
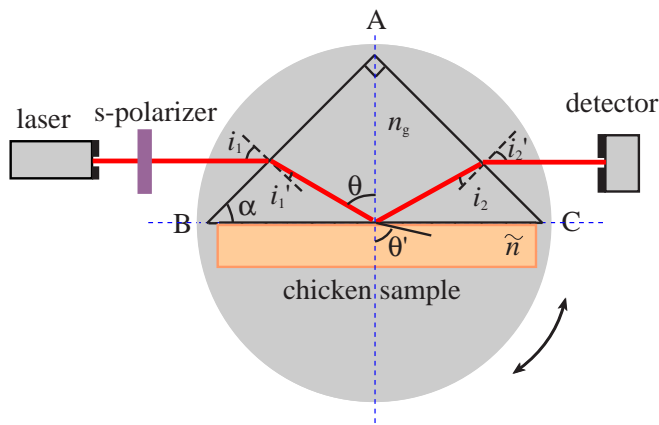
FIG. 1 Schematic of the experimental setup for measuring the refractive index.

tude as the wavelength. Note that the mean-free-path is about 100 μm for most tissue types, which is much longer than the wavelengths available [10]. Thus, when total internal reflection takes place, statistically significant scattering does not occur if the tissue is used as the second medium. We adopted this approach to measure the coherent transmittivity T_s of an s-polarized incident wave of a tissue-prism system as a function of the incident angle i_1 from the interface between air and a glass prism. The measured coherent transmittivity was fitted with the calculated values from the Fresnel equations, which require the assumed value of the complex refractive index of the sample $\tilde{n} = n - ik$ and the known refractive index n_g of the prism. The value of $\tilde{n}$ was inversely determined by using an iteration process to achieve the least-squares difference between the measured and the calculated T_s. A schematic of the optical setup was shown in Figure 1. A collimated s-polarized laser beam of power I with an incident angle of i_1 was incident on one side AB of a right-angle prism, which was placed on a goniometer rotated by a step motor. It then was refracted with a refractive angle of i_1'. Next, light with an incident angle of θ irradiated the interface BC between the prism base and tissue sample. The reflected beam propagated along the specular reflection angle and exited symmetrically from the other side surface AC of the prism, and its power I could be measured with a photodiode. The total coherent transmittivity T_s was equal to I/I_0.

According to the Fresnel equations, the reflectivity of planes AB, BC, and AC for s-polarized incident waves can be given by

$$R_{AB} = \left[\frac{\sin(i_1 - i_1')}{\sin(i_1 + i_1')}\right]^2 \tag{1a}$$

$$R_{BC} = \left[-\frac{\sin(\theta - \theta')}{\sin(\theta + \theta')}\right]^2 \tag{1b}$$

$$R_{AC} = \left[\frac{\sin(i_2 - i_2')}{\sin(i_2 + i_2')}\right]^2, \tag{1c}$$

where $i_1, i_1', \theta, \theta', i_2, i_2'$ are the incident angles and refractive angles of the planes AB, BC, and AC, respectively. Given the assumptions that the prism angle is α (here $\alpha = 45°$) and the refractive index of the ambient medium is n_0 (here $n_0 = 1$), there are the following relationships according to Snell's law

and simple geometric relationships,

$$n_0 \sin i_1 = n_g \sin i_1' \tag{2a}$$

$$n_g \sin i_2 = n_0 \sin i_2' \tag{2b}$$

$$n_g \sin \theta = \tilde{n} \sin \theta' \tag{2c}$$

$$\theta = i_1' + \alpha \tag{2d}$$

$$i_2 = \theta - \alpha, \tag{2e}$$

where $\tilde{n}$ is the reflective index of the tissue sample. Therefore, the total coherent transmittivity T_s of an s-polarized incident wave can be calculated by

$$T_s = (1 - R_{AB})R_{BC}(1 - R_{AC}). \tag{3}$$

The complex refractive index $\tilde{n}$ of tissue is solved with a method of least squares based on the Marquardt–Levenberg nonlinear regression algorithm by fitting the calculated values T_s to the measured values. Theoretically, $\tilde{n}$ can be solved from Eqs. (1)–(3). However, it is problematic to obtain a convergent, stable and accurate solution because of the complex $\tilde{n}$. To avoid this problem, we have chosen to use the following simple analytical expression of reflectivity of an s-polarized incident wave of plane BC given by Humphreys-Owen [8]:

$$R_{BC}' = \frac{M + x^2 - x\sqrt{2(M + L)}}{M + x^2 + x\sqrt{2(M + L)}}. \tag{4}$$

If the complex refractive index of tissue relative to the prism is

$$N_r = \frac{\tilde{n}}{n_g} = \frac{n}{n_g} - \frac{k}{n_g}i = N_1 - N_2i, \tag{5}$$

then $L = N_1^2 - N_2^2 - y^2$, and $M^2 = L^2 + 4N_1^2N_2^2$, where $x = \cos\theta$ and $y = \sin\theta$. Thus, Eq. (3) can be rewritten as

$$T_s = \left\{1 - \left[\frac{\sin(i_1 - i_1')}{\sin(i_1 + i_1')}\right]^2\right\} \times \left[\frac{M + x^2 - x\sqrt{2(M + L)}}{M + x^2 + x\sqrt{2(M + L)}}\right]$$
$$\times \left\{1 - \left[\frac{\sin(i_2 - i_2')}{\sin(i_2 + i_2')}\right]^2\right\}. \tag{6}$$

Plots of T_s versus i_1 show the effects of sample absorption and scattering on T_s for various values of n and k. Figure 2 shows
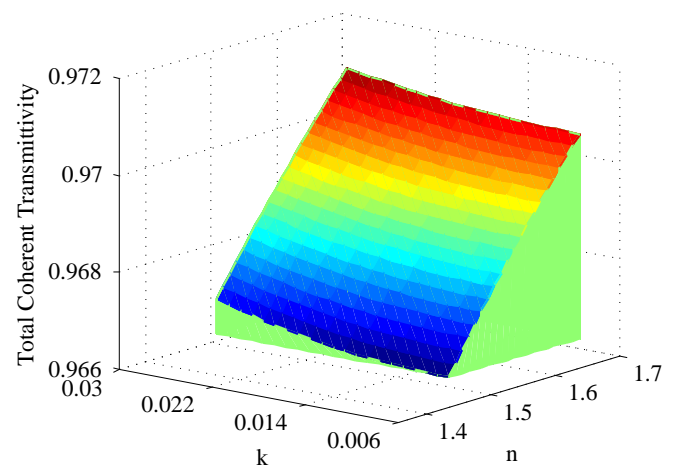

FIG. 2 The 3-dimensional curve of the total coherent transmittivity relative to various real and imaginary parts of the refractive indices (incident angle $i_1 = 10°$).
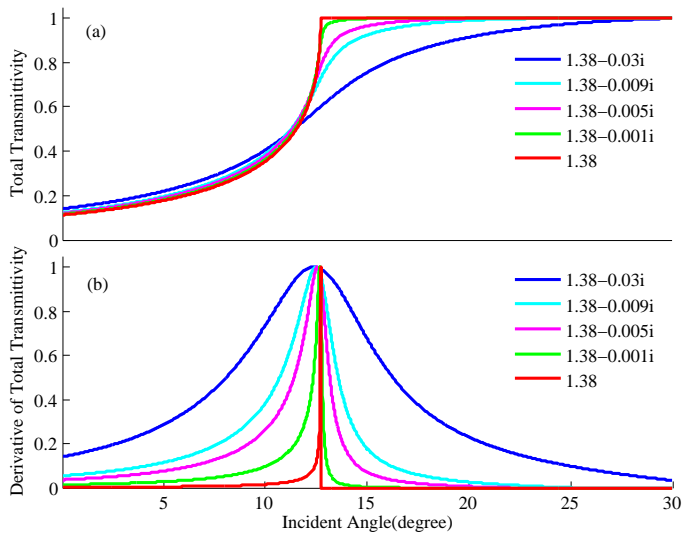
FIG. 3 The relationship between the total coherent transmittivity curves (a) and their derivatives (b) for various imaginary parts of refractive indices.
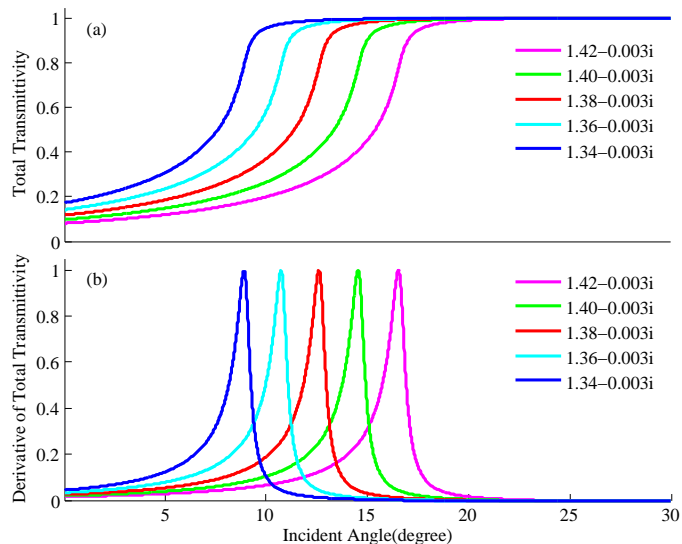

FIG. 4 The relationship between the total coherent transmittivity curves (a) and their derivatives (b) for various real parts of refractive indices.

the 3-dimensional curve of T_s relative to various n and k (set $i_1 = 10°$, $n_g = 1.7453$, $\alpha = 45°$, $n_0 = 1$). Note that transmittivity increases as n and k increase.

Figure 3 shows the relationship between the transmittivity curves and their derivatives for various values of k. Note that the transmittivity curve at a critical illumination angle changes sharply at $k = 0$ and gradually when $k > 0$. For a non-absorbing or non-scattering medium (i.e., $k = 0$), the angular positions of the maximum derivatives of the transmittivity curves are the same as the critical angle. However, for an absorbing or scattering medium (i.e., $k > 0$), the angular positions of the maximum derivatives of the transmittivity curves deviate from the critical angle.

Figure 4 shows the relationship between the transmittivity curves and their derivatives for various values of n. Note that the shift in the transmittivity curve is sensitive to different val-

ues of n; therefore, the accuracy of this curve-fitting method is high.

3 RESULTS

Fresh chicken tissues were obtained from the chest area of five different domestic 2 month old chickens from a slaughterhouse. The obvious fibrous structure of the tissue was suitable for this study of optical anisotropy. The chicken patches were stored in a bucket on crushed ice ($\sim 0°C$) in a refrigerator immediately after removal from the chickens. The sample sections were prepared so that they were approximately 2 mm thick, 10 mm wide, and 20 mm long. They were warmed naturally to room temperature ($\sim 20°C$). First, the base surface of a 20×40 cm prism was smeared with refractive index matching liquid (Mycro Technologies Co., Ltd., the refraction index was 1.7452). Then, the section was softly stuck to the base surface. In this way, some air bubbles due to the rough surface of tissue [20] were eliminated. The pressure effect caused by pressing the section against the base surface [21] was also cancelled.

The experimental setup was similar to that shown in Figure 1. In all experiments described below, we used the same semiconductor laser (40 mW; 650 nm; beam divergence < 0.3 mrad) at room temperature. *S*-polarized light was used to measure the refractive index of the tissue samples. The collimated laser beam irradiated one side of a right-angle glass prism (ZF6, $n_g = 1.7453$) through an *s*-polarizer with an aperture of 1.5 mm. The prism was attached to a rotated goniometer driven by a rotation stage with an angle resolution of $1'$. When the incident angle was changed, a photodiode received the power of the light emitted out of another side of the prism. To calibrate the experimental apparatus, first, we measured the T_s curve of deionized water. The value of real refractive index of deionized water was 1.3289 and the imaginary index was less than 8×10^{-5}. This value was close to that of Li and Xie's work [10] (H_2O, $n = 1.322 \pm 0.006$, 632.8 nm).

Then, we measured the refractive index of the chicken tissue sections. To investigate optical anisotopy, we selected five chicken tissue sections each from different chickens. In addition, we altered three angles for each section with linearly *s*-polarized light incident upon the tissue sample, with electric fields directed parallel, perpendicular, and 45° to the measured fiber orientation. The angle was denoted as Φ and assigned as 0°, 90°, and 45°. Five time measurements were carried out for each section and for each angle and the last value was the average. Figure 5 shows three total coherent transmittivity curves for $\Phi = 0°$, 45°, 90° that were measured, which fit the theoretical curves well. Table 1 shows the detailed values for three indices. Note that the refractive index at 0° is the

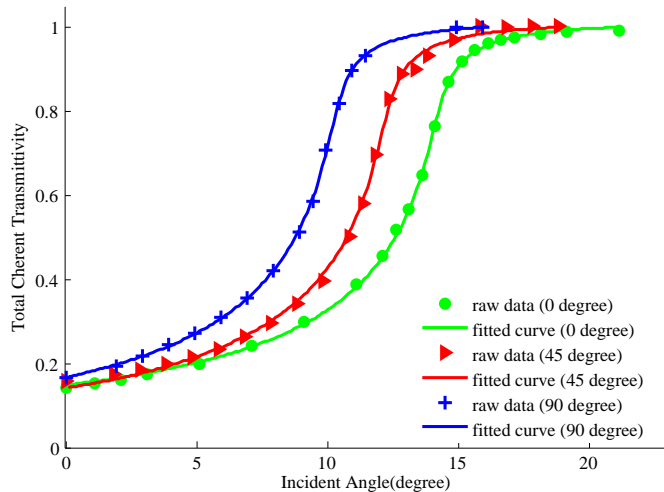| Φ	$\tilde{n} = n - ik$
0°	$1.3949 - 0.0053i$
45°	$1.3746 - 0.0054i$
90°	$1.3540 - 0.0053i$

TABLE 1 Results for the refractive indices of chicken tissues

FIG. 5 The total coherent transmittivity curves that were measured at different angles, and the fitted curves.

FIG. 6 Construction of polarized light coherence.

highest, that at 90° is the lowest, and that at 45° is almost the average of the sum of the reflective indices at 0° and 90°.

4 DISCUSSION

Three issues should be considered in an assessment of these results. The first concern is the meaning of refractive index. From the point of view of electromagnetic waves, the real part of the refractive index shows the phase retardation of the wave caused by tissue, and the imaginary part shows the attenuation. The total attenuation coefficients, as the sum of the scattering and absorption, appear to affect the imaginary refractive index of chicken tissue significantly, as shown in Figures 3 and 5. The diffuse scattering originates from two sources: the rough tissue surface mismatched optically with the prism glass and the tissue bulk. However, the diffuse scattering should be dominated by the light scattering in the tissue bulk [11]. The water, hemoglobin and other chromophores in the tissue are the primary factors that affect the absorption in the visible and near infrared ranges. The result of the imaginary refractive index (in orders of 10^{-3}), as shown in Table 1, is much less than that of the real refractive index. One explanation might be the light color of the chicken tissue. The imaginary refractive index of the dark tissues like liver and kidney may be greater than that of chicken tissue in quantity.

The second concern is the anisotropy refractive index. We used a construction of polarized light coherence [22], as shown in Figure 6, to confirm the optical axis of the chicken tissue. The chicken tissue sections that were 0.1 mm thick, 20 mm wide, and 40 mm long were fabricated using the above method. The absorption and scattering effects can be neglected because the section was thin. The section was located between two orthogonal linear polarizers. P as a polarizer ensured that the linear *s*-polarization of the input laser and A as an analyzer tested the polarization state of exiting light. The tissue section was rotated between 0° and 90°. When the fiber orientation of the tissue section was parallel to the vibrating direction of the electric field of P, the exiting intensity was at its minimum. In accordance with the
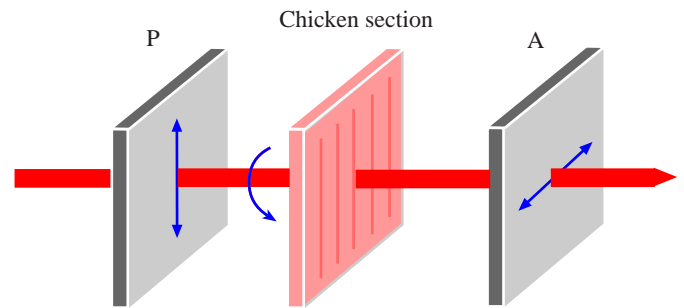
coherent principle of polarized light [22], the fiber orientation is the direction of the optical axis of the tissue. Because the electric displacement vector of the ordinary wave vibrates perpendicular to the principal plane (the plane containing the wave normal and the optical axis), the electric displacement vector of the extraordinary wave vibrates in the principal plane [22]. Thus, the fiber orientation is the vibrating direction of the electric displacement vector of ordinary light. The tissue section is similar to a negative uniaxial crystal wafer. The refractive index measured at $\Phi = 0°$ was that of an ordinary wave, i.e. n_o, and the refractive index measured at $\Phi = 90°$ was that of an extraordinary wave, i.e. n_e. Here, $n_o = 1.3949 + 0.0053i$ and $n_e = 1.3540 + 0.0053i$. It is known that the real part of n_o is larger than that of n_e, but both the imaginary parts of n_o and n_e are the same within the measurement limits of this study. The refractive index of the chicken tissue was higher along the length of fibers than that along the cross section. This important conclusion is in agreement with other studies [14, 15].

Last, the uncertainty in the experimental data, i.e., the sum of the squared standard deviations, should be assessed. The main sources of measurement uncertainty originate from three factors. The first was the accuracy of the goniometer, which was restricted within 1′. The error can be estimated as ±0.0002 from the angle of total reflectance [23]. The second was the small difference in the refractive indices between the prism and refractive index matching liquid. The gap was only 0.0001, so the error was estimated at ±0.00007. The third was the curve-fit deterioration that was due to statistical error in the raw data. A method based on Matlab was proposed to estimate the curve-fit error in this study. This method is described in detail below. A new matrix was generated by multiplying the "raw data" with an artificial matrix of pseudo-random numbers. Given the assumption that the squared standard deviations between the new matrix and the "raw data" matrix was equal to that between the "raw data" matrix and curve-fit, the statistical error of the refractive index was the squared standard deviations of nonlinear regression from the new data and the raw data. In this way, the statistical error was estimated at ±0.00002. Table 2 shows the uncertainty of the refractive indices originating from the three main sources. As a whole, the maximum absolute error and relative error of the measurement data were about ±0.0003 and 0.02%, respectively. The results indicated that the measurement accuracy of this study was high.

Source	Maximum of absolute errors	Maximum of relative errors
accuracy of goniometer	±0.0002	0.01%
difference of refractive indices	±0.00007	0.005%
curve-fit	±0.00002	0.001%

TABLE 2 Sources of uncertainty.

5 CONCLUSIONS

We used the specular reflection method to study the anisotropy complex refractive index of chicken tissue at 650 nm. Our results are described well by Fresnel's theory. Analysis of the data indicates that the chicken tissue with fibrous structures showed optical anisotropy. The refractive index was higher along the orientation of the fibers than along the cross section. Furthermore, the refractive index along the orientation of fibers was that of an ordinary wave and the refractive index along the cross section was that an extraordinary wave. The fiber orientation was in the direction of the optical axis of the chicken tissue and the chicken tissue section was similar to a negative uniaxial crystal wafer. Therefore, all of tissues with apparent fibrous structures possibly present optical anisotropy. In this study, the refractive indices were measured at 650 nm, but the method and measurement skills of this work could also be applied to other wavelengths.

6 ACKNOWLEDGEMENTS

References

[1] B. C. Wilson, and M. S. Patterson, "The physics, biophysics and technology of photodynamic therapy" Phys. Med. Biol. **53**, R61–R109 (2008).

[2] D. A. Benaron, "The future of cancer imaging" Cancer Metast. Rev. **21**, 45–78 (2002).

[3] X. Ma, J. Q. Lu, R. S. Brock, K. M. Jacobs, P. Yang, and X. H. Hu, "Determination of complex refractive index of polystyrene microspheres from 370 to 1610 nm" Phys. Med. Biol. **48**, 13–27 (2003).

[4] L. H. Wang, S. L. Jacuues, and L. Q. Zheng, "MCML—Monte Carlo modeling of light transport in multi-layered tissues" Comput. Meth. Prog. Bio. **47**, 131–146 (1995).

[5] X. X. Guo, M. F. G. Wood, and A. Vitkin, "Monte Carlo study of path length distribution of polarized light in turbid media" Opt. Express **15**, 1348–1360 (2007)

[6] F. P. Bolin, L. E. Preuss, R. C. Taylor, and R. J. Ference, "Refractive index of some mammalian tissues using a fiber optics cladding method" Appl. Opt. **28**, 2297–2303 (1989).

[7] A. Knüttel, and M. Boehlau-Godau, "Spatially confined and temporally resolved refractive index and scattering evaluation in human skin performed with optical coherence tomography" J. Biomed. Opt. **5**, 83–92 (2000).

[8] G. H. Meeten, and A. N. North, "Refractive index measurement of absorbing and turbid fluids by reflection near the critical angle" Meas. Sci. Technol. **6**, 214–221 (1995).

[9] Y. Räty, E. Keräneny, and K.-E. Peiponen, "The complex refractive index measurement of liquids by a novel reflectometer apparatus for the UV–visible spectral range" Meas. Sci. Technol. **9**, 95–99 (1998).

[10] H. Li, and S. S. Xie, "Measurement method of the refractive index of biotissue by total internal reflection" Appl. Opt. **35**, 1793–1795 (1996).

[11] H. Ding, J. Q. LU, W. A. Wooden, P. J. Kragel, and X. H. Hu, "Refractive indices of human skin tissues at eight wavelengths and estimated dispersion relations between 300 and 1600 nm" Phys. Med. Biol. **51**, 1479–1489 (2006).

[12] Y. L. Jin, J. Y. Chen, L. Xu, and P. N. Wang, "Refractive index measurement for biomaterial samples by total internal reflection" Phys. Med. Biol. **51**, N371–379 (2006).

[13] P. Sun, and Y. Wang, "Measurements of optical parameters of phantom solution and bulk animal tissues in vitro at 650 nm" Opt. Laser Technol. **42**, 1–7 (2010).

[14] X. Wang, and L. V. Wang, "Propagation of polarized light in birefringent turbid media: time-resolved simulations" Opt. Express. **9**, 254–259 (2001).

[15] X. Wang, and L. V. Wang, "Propagation of polarized light in birefringent turbid media: A Monte Carlo study" J. Biomed. Opt. **7**, 279–290 (2002).

[16] J. F. de Boer, T. E. Milner, M. J. C. van Gemert, and J. S. Nelson, "Two-dimensional birefringence imaging in biological tissue by polarization-sensitive optical coherence tomography" Opt. Lett. **22**, 934–936 (1997).

[17] K. Schoenenberger, B. W. Colston, D. J. Maitland, L. B. Da Silva, and M. J. Everett, "Mapping of birefringence and thermal damage in tissue by use of polarization-sensitive optical coherence tomography" Appl. Opt. **37**, 6026–6036 (1998).

[18] C. K. Hitzenberger, E. Götzinger, M. Sticker, M. Pircher, and A. F. Fercher, "Measurement and imaging of birefringence and optic axis orientation by phase resolved polarization sensitive optical coherence tomography" Opt. Express. **9**, 780–790 (2001).

[19] B. Liu, M. Harman, S. Giattina, D. L. Stamper, C. Demakis, M. Chilek, S. Raby, and M. E. Brezinski, "Characterizing of tissue microstructure with single-detector polarization-sensitive optical coherence tomography" Appl. Opt. **45**, 4464–4479 (2006).

[20] X. Y. Ma, J. Q. Lu, and X. H. Hu, "Effect of surface roughness on determination of bulk tissue optical parameters" Opt. Lett. **28**, 2204–2206 (2003).

[21] V. V. Tuchin, "Immersion effects in tissues" Proc. SPIE **4162**, 1–19 (2000).

[22] M. Born, and E. Wolf, *Principles of Optics* pp. 823–826 (London University Press, London, 1999).

[23] J. C. Lai, Z. H. Li, C. Y. Wang, and A. Z. He, "Experimental measurement of the refractive index of biological tissues by total internal reflection" Appl. Opt. **44**, 1845–1849 (2005).